ChemPubSoc Europe

DOI: 10.1002/chem.201802147

CHEMISTRY A European Journal Full Paper

DNA Recognition

Binding Modes and Selectivity of Ruthenium Complexes to Human Telomeric DNA G-Quadruplexes

Jenifer Rubio-Magnieto,[a, g] Sofia Kajouj,[b] Florent Di Meo,[c] Mathieu Fosséprè,[a] Patrick Trouillas,[c, d] Patrick Norman,[e] Mathieu Linares,[e, f] Cécile Moucheron,*[b] and Mathieu Surin*[a]

Abstract: Metal complexes constitute an important class of DNA binders. In particular, a few ruthenium polyazaaromatic complexes are attractive as "light switches" because of their strong luminescence enhancement upon DNA binding. In this paper, a comprehensive study on the binding modes of several mononuclear and binuclear ruthenium complexes to human telomeric sequences, made of repeats of the d(TTAGGG) fragment is reported. These DNA sequences form G-quadruplexes (G4s) at the ends of chromosomes and constitute a relevant biomolecular target in cancer research. By combining spectroscopy experiments and molecular modelling simulations, several key properties are deciphered: the binding modes, the stabilization of G4 upon binding, and the selectivity of these complexes towards G4 versus double-stranded DNA. These results are rationalized by assessing the possible deformation of G4 and the binding free energies of several binding modes via modelling approaches. Altogether, this comparative study provides fundamental insights into the molecular recognition properties and selectivity of Ru complexes towards this important class of DNA G4s.

[a] *Dr. J. Rubio-Magnieto, Dr. M. Fosséprè, Prof. M. Surin*
Laboratory for Chemistry of Novel Materials
Center for Innovation in Materials and Polymers
University of Mons-UMONS
20 Place du Parc, 7000 Mons (Belgium)
E-mail: mathieu.surin@umons.ac.be

[b] *Dr. S. Kajouj, Prof. C. Moucheron*
Chimie Organique et Photochimie CP160/08
Université libre de Bruxelles
50 avenue F. D. Roosevelt, 1050 Bruxelles (Belgium)
E-mail: cmouche@ulb.ac.be

[c] *Dr. F. Di Meo, Prof. P. Trouillas*
INSERM U1248 IPPRITT, University of Limoges
School of Pharmacy, 2 rue du Dr. Marcland, 87025 Limoges (France)

[d] *Prof. P. Trouillas*
RCPTM, Palacký University
Faculty of Sciences, Šlechtitelů 27, 78371 Olomouc (Czech Republic)

[e] *Prof. P. Norman, Dr. M. Linares*
Department of Theoretical Chemistry and Biology
School of Engineering Sciences in Chemistry
Biotechnology and Health
KTH Royal Institute of Technology
SE-106 91 Stockholm (Sweden)

[f] *Dr. M. Linares*
Swedish e-Science Research Centre (SeRC)
KTH Royal Institute of Technology
104 50 Stockholm (Sweden)

[g] *Dr. J. Rubio-Magnieto*
Current address: Bioinspired Supramolecular Chemistry and Materials group
Departament de Química Inorgànica i Orgànica
Universitat Jaume I, Avda Sos Baynat s/n, E-12071, Castelló (Spain)

Supporting information and the ORCID identification number(s) for the author(s) of this article can be found under: https://doi.org/10.1002/chem.201802147.

Introduction

Specific Guanine-rich DNA sequences can form four stranded structures called G-quadruplexes (G4s), which were first described by Gellert et al. in 1962.[1] G4 structures involve stacks of G-quartets formed by the association of four guanine bases in a plane, linked together by Hoogsteen hydrogen bonds. Monovalent cations, such as K^+ or Na^+, can stabilize G4 structures by coordinating the oxygen of the carbonyl groups. There exists compelling evidence that DNA G4s are formed in human cells,[2] in particular at the ends of chromosomes that are known as telomere regions and in the transcriptional regulatory regions of many oncogenes, and which therefore makes them very interesting biomolecular targets. Indeed, the telomere regions in all vertebrates are composed of a repetition of a G-rich DNA sequence, namely $d(TTAGGG)_n$.[3] Although the majority of telomeric DNA is double stranded, the 3′ extremity is a guanine rich single strand known as G-overhang, and the length of this single-strand varies between species from 12 to several hundred repeat units.[4] Telomeres have a protective role against events causing genetic instability that result in damage, recombination, or inter-chromosomal fusions.[5] Telomeres also protect the genetic material during cell division and are linked to the limited potential for a cell to replicate. Indeed, in human somatic cells, telomeres are shortened with each cell division with about 50 to 200 bases, due to the inability of the DNA polymerase to fully replicate. When the erosion limit is reached, the cell cannot continue to divide and enters a state of senescence. However, maintenance mechanisms of these telomeres exist that reverse this gene shortening effect

and thus increase the cell replication capacity. In human cells, the function of telomerase is to add multiple copies of 5′-GGTTAG-3′ sequence. The telomeric end with its guanine-rich single strand seems particularly suitable for the formation of G4 structures. Indeed, it has been demonstrated that the formation of G4 structures in the telomeric single strand region can inhibit telomerase activity and this makes them important as therapeutic targets.[6]

The search for new molecules able to stabilize G4s has become an active field of research in anti-cancer drug design.[7] This includes notably planar π-conjugated molecules,[8] porphyrins and phthalocyanine derivatives,[6c,9] and coordination complexes.[10] It has been demonstrated that coordination complexes (e.g., with Ru^{II}, Ni^{II}, Zn^{II}, Mn^{III} metal centers) can strongly and selectively interact with DNA G4.[10b,11] Indeed, Ru complexes offer potential benefits in the field of medicinal chemistry because of their notable interactions with DNA.[12] For instance, the well-known $[Ru(bpy)_2dppz]^{2+}$ (bpy = 2,2′-bipyridine; dppz = dipyrido[3,2-*a*:2′,3′-*c*]phenazine), known as a "*light switch*", was shown to intercalate in between DNA base pairs by means of its planar ligand ddpz.[13] Recent results highlighted a light-switch effect with human telomeric DNA sequences, where this metal complex showed a preferential binding to G4 structures (stabilized by Na^+ or K^+) over an i-motif.[14] Its analogue, $[Ru(phen)_2dppz]^{2+}$ (phen = 1,10-phenanthroline) also demonstrated an ability to stabilize G4 structures.[11d,15] Since the ionic strength around the G4 structure is more important than the one around DNA duplexes,[16] bi- or multi-nuclear complexes seem to be promising candidates to efficiently interact with G4. For example, the binuclear complex $[(bpy)_2Ru(tpphz)Ru(bpy)_2]^{4+}$ (tpphz = tetrapyridophenazine) can induce an anti-parallel G4 formation in the absence of alkali cations.[17] The two isomers of the binuclear ruthenium complex $[(Ru(phen)_2)_2tpphz]^{4+}$, which possess the same affinity to duplex DNA, are other examples that show enantioselective binding with G4 structures.[18] In this context, we previously designed a binuclear complex $[(TAP)_2Ru(TPAC)Ru(TAP)_2]^{4+}$ (TAP = 1,4,5,8-tetraazaphenanthrene; TPAC = tetrapyrido[3,2-*a*:2′,3′-*c*:3″,2″-*h*:2‴,3‴-*j*]acridine) able to photo-react with DNA duplexes and G4s; the photo-crosslinks between the TAP ligands and the guanine bases strongly stabilize a human telomeric sequence G4, a key point to inhibit the telomerase activity.[19]

In this paper, we report a comprehensive study of the binding modes and selectivity of a series of Ru complexes potentially able to interact with DNA G4, in particular G4 forms of the human telomeric sequence. We aim at identifying the complexes with the highest potential for interaction and stabilization of these biomolecular targets. To achieve this goal, different types of complexes have been studied (Scheme 1): homoleptic complexes such as **$[Ru(TAP)_3]^{2+}$** and **$[Ru(phen)_3]^{2+}$**, and heteroleptic complexes **$[Ru(phen)_2PHEHAT]^{2+}$** (PHEHAT = 1,10-phenanthrolino[5,6-*b*]-1,4,5,8,9,12-hexaazatriphenylene) with an extended planar ligand and its binuclear analogue **$[(phen)_2RuPHEHATRu(phen)_2]^{4+}$**. This series allows us to decipher the structural parameters driving the Ru complex specificity towards human telomeric G4. The Ru complexes studied here are in the form of mixtures of optical isomers (i.e., mixtures of Δ and Λ for mononuclear complexes, and ΔΔ, ΛΛ, ΛΔ for the binuclear complex), and this study is focused more particularly on the differences of binding for complexes of different shapes and charges. By combining complementary experimental and computational approaches, this study provides new insights into the binding modes, recognition mechanisms, affinity, and selectivity of various Ru complexes towards DNA G4s.

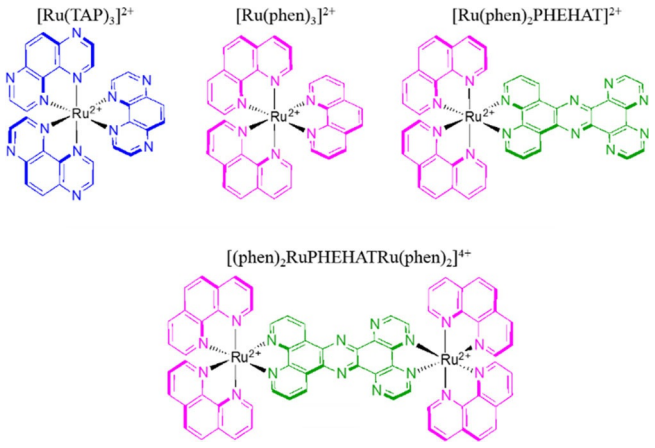

Scheme 1. Chemical structures of the Ru complexes under study: $[Ru(TAP)_3]^{2+}$, $[Ru(phen)_3]^{2+}$, $[Ru(phen)_2PHEHAT]^{2+}$, and $[(phen)_2RuPHEHATRu(phen)_2]^{4+}$.

Experimental Section

Synthesis and Characterization: $[Ru(phen)_3]^{2+}\cdot 2Cl^-$ is commercially available and was purchased from Sigma Aldrich, $[Ru(TAP)_3]^{2+}\cdot 2Cl^-$, $[Ru(phen)_2PHEHAT]^{2+}\cdot 2Cl^-$ and the binuclear $[(phen)_2Ru\text{-}PHEHAT\text{-}Ru(phen)_2]^{4+}\cdot 4Cl^-$ were synthetized according to procedures described in the literature.[20–22] All of the chemicals and solvents (reagent grade quality or HPLC grade) were used without further purification. All of the reaction mixtures were protected from direct light during the synthesis to prevent photochemical degradation. Oligonucleotides (ODNs) were purchased from Eurogentec (Belgium) with the highest purity grade (UltraPureGold™, RP -HPLC, >95% pure in sequence) and the composition of ODNs was checked by MALDI-ToF. A Tris-EDTA buffer (TE buffer) at pH 7.4 was prepared by using 10 mM Tris (tris(hydroxymethyl)aminomethane), 1 mM EDTA, and MilliQ water. Each ODN was dissolved in a volume of TE buffer at a concentration of 100 μM (expressed per strand). After addition of the buffered solution, the ODN samples were centrifuged during 2 min at 2000 rpm. Small volumes of this solution were used to prepare different aliquots, on which were added TE buffer, or TE buffer + KCl (3 M) or + NaCl (3 M) in order to obtain a final volume of 300 μL and solutions in pure TE buffer or TE buffer + 100 mM K^+ ions or TE buffer + 100 mM Na^+ ions, respectively. The solution was then mixed using a vortex mixer. The concentration of the aliquot of ODN in the buffer solution was determined by UV/Vis at 25 °C using the specific extinction coefficient at 260 nm (ε_{260}) of Tel22 ($d[AG_3(T_2AG_3)_3]$), which is 228500 $L\,mol^{-1}\cdot cm^{-1}$. The Ru complexes were also dissolved in TE buffer (pH 7.4, 10 mM Tris buffer and 1 mM EDTA) or in TE buffer + 100 mM KCl or NaCl and the molar ratio between Ru-complexes and DNA was adjusted using the calculated molar concentrations of DNA (around 7 μM). The solutions of Ru complexes were added

to the DNA solutions and were stirred using a vortex during 2 min and allowed to equilibrate for 30 min.

UV/Vis absorption and Circular Dichroism spectroscopy: The UV/Vis absorption and Circular Dichroism (CD) measurements were recorded using a Chirascan™ Plus CD Spectrometer from Applied Photophysics. The measurements were carried out using 2 mm suprasil quartz cells from Hellma Analytics. The spectra were recorded at 5 °C (temperature at which the equilibrium was strongly shifted towards the folded forms) between 210 and 650 nm, with a bandwidth of 1 nm, time per point 1 s and 2 repetitions. The buffered water solvent reference spectra were used as baselines and were automatically subtracted from the CD spectra of the samples.

Fluorescence Resonance Energy Transfer (FRET) melting assays: FRET melting assays were performed according to Mergny et al.,[23] using a synthetic double-dye labelled oligonucleotide called **F21T** 5′-FAM-GGG(T_2AG_3)$_3$-TAMRA-3′ (purchased from Eurogentec, Belgium). The solutions were prepared at a concentration of around 0.3 μM (ODN concentration) in 10 mM lithium cacodylate buffer (pH 7.2) in presence of 10 mM KCl + 90 mM LiCl (K^+ medium) or in presence of 100 mM NaCl (Na^+ medium). The solutions were first heated to 90 °C for 3 min in the corresponding buffer conditions and then put on ice to support the formation of G4 secondary structure. For preparing the mixtures, the Ru complexes were added at concentrations of around 1 μM and 3 μM, to reach molar ratios of 1:3 and 1:10 in **F21T**:Ru complex, respectively. The mixtures were equilibrated at 25 °C during 5 min. The FRET spectra were measured using a Chirascan™ Plus CD Spectrophotometer equipped for fluorescence measurements. The samples were excited at 492 nm and the fluorescence emission spectra were collected between 500 and 700 nm. The temperature was varied from 25 °C to 96 °C at a rate of 1 °C min^{-1}. The melting of the **F21T** was monitored by measuring the fluorescence of FAM (at 516 nm), as described in Ref. [23]. The FAM emission intensity was normalized and $\Delta T_{1/2}$ was defined as the temperature for which the normalized emission equals 0.5. For the selectivity studies, a solution of 10 molar equivalents of a dsDNA competitor (≈3 μM in double-strand) was added into the **F21T**/Ru complex solution and the final solution was equilibrated at 25 °C during 5 min. The dsDNA competitor (**ds26)** is a 26 base pairs with sequence: 5′-CAATCGGATCGAATTCGATCCGATTG-3,′ hybridized with its complementary sequence (purchased from Eurogentec).

Luminescence lifetime measurements. Luminescence lifetime were determined by Time-Correlated Single Photon Counting (TCSPC) using an Edinburgh Instruments LifeSpec-II equipped with F900 CDT software. The instrument includes a laser diode (PDL445) as excitation source for which the laser pulse length is lower than 100 ps. The Hamamatsu R3809U-50 detector possesses an intrinsic instrumental response lower than 25 ps and a spectral coverage from 250 to 850 nm. In normal measurement conditions, the background noise is about 10 shots. The experimental data were fitted by a multi-exponential decay as described by Equation (1):

$$I(t) = A + \sum_i B_i exp^{\left(\frac{-t}{\tau_i}\right)} \quad (1)$$

with A, an arbitrary constant; B_i, a pre-exponential factor proportional to the quantity of i species with a luminescence lifetime τ_i. The percentages of different luminescence lifetimes τ_i, are given by the ratio of pre-exponential factors, $\%_i = \frac{B_i}{\sum_i B_i}$. When experimental data are fitted with multi-exponential decay, an average luminescence lifetime, as described in the equation below, can be used to discuss the data. $\tau_m = \frac{\sum_i (B_i \times \tau_i)}{\sum_i B_i}$ Ru complexes were also dissolved in TE buffer (pH 7.4, 10 mM Tris buffer and 1 mM EDTA) + 100 mM KCl or NaCl and the molar ratio between Ru-complexes and DNA was adjusted using the calculated molar concentrations of DNA. The solution of Ru complexes was added to the DNA solution and was stirred using a vortex at vigorous speed during 2 min and allowed to equilibrate for 30 min.

Molecular modelling and simulations: Force field parameters of **[Ru(phen)$_3$]$^{2+}$** and **[Ru(phen)$_2$PHEHAT]$^{2+}$** were derived from GAFF[24] and quantum-chemical calculations at the B3LYP/6–31 + G(d,p)/LANL2DZ level. The LANL2DZ effective core potential was used for ruthenium and the all electron 6–31 + G(d,p) basis set for carbon, nitrogen and hydrogen. Parameters of bonds, angles and dihedral angles involving Ru were derived from the work of Norrby et al.[25] and which were later also used by Rothlisberger et al.[26] and Thomas et al.[18] Optimized geometries were used to calculate the RESP (Restricted ElectroStatic Potential) partial atomic charges at the Hartree–Fock level of theory with the basis set described above. The Ru partial atomic charge depends strongly on the adopted level of theory, and it was fixed at +1.41e during the RESP calculation in agreement with the previous work of Thomas et al.[18] The adopted Tel22 antiparallel and hybrid G4 structures were initially obtained from the PDB database (PDB ID: 143D and 2H79)[27] and further optimized in our previous work.[9d] The AMBER ff99SBbsc0 force field[28] was used to model the G4 structures. Water molecules were described with the TIP3P model.[29] The cut-off distances for explicit Coulombic and van der Waals' interactions were set to 12 Å and the size of box was chosen as to avoid self-interactions. Molecular dynamics (MD) simulations were performed on pure G4 structures as well as 1:1 G4:**[Ru(phen)$_3$]$^{2+}$** and G4:**[Ru(phen)$_2$PHEHAT]$^{2+}$** complexes. For each 1:1 G4:Ru complex to be modeled, between four and six binding modes (or starting points) were initially considered (as detailed in the Supplementary Information). A box with pure water used for solvation was initially equilibrated in a 100 ps long (*N*,*P*,*T*)-MD simulation, resulting in a density of 0.99 g cm^{-3}. Then, unbiased (*N*,*P*,*T*)-MD simulations were carried out for 200 and 300 ns, respectively, for solvated G4 structures and solvated 1:1 G4:Ru complexes. The particle mesh Ewald (PME) MD simulations were carried out using the SHAKE algorithm. The temperature was maintained using the Langevin thermostat with a collision frequency of 1 ps^{-1}. Isotropic pressure scaling was used in which the pressure relaxation time was set at 1 ps, using the Berendsen barostat. Conformational analyses were carried out using the cpptraj software over the last 100 ns.[30] The theoretical assessment of DNA unbinding free energy (ΔG_{unbind}) between Ru complexes and DNA was performed using potential of mean force (PMF) calculations. For each conformation, 100 constant-velocity steered MD (SMD) simulations were carried out from 10 different replicas extracted from the last 50 ns of the unbiased MD simulations. For each SMD, Ru-based ligands were pulled away from G4. Using a harmonic bias potential by which the force constant was set at 7.2 kcal mol^{-1} Å^{-2} and applied to the distance between the centers of mass of (i) Ru-ligand and (ii) DNA interacting with Ru-ligand at a pulling velocity of 1 m s^{-1} (or 10 Å ns^{-1}). This allowed the use of a rather limited number of samples (i.e., 100 replicas per system).[31] The binding free energies were assessed according to the isobaric-isothermal Jarzynski equality,[32] that is, $\langle e^{-\beta W} \rangle = e^{-\beta \Delta G}$. Statistics on free energy calculations was obtained from the block average of ten blocks of ten trajectories.[33] It is important to note that absolute free energies are only discussed semi-quantitatively owing to the questionable robustness of absolute binding free energies calculated by steered MD. However, since the bias arising from steered MD is the same for every system, this approach is considered reliable for relative comparisons made to *rank* the dif-

ferent binding modes. The total MD simulation time for PMF calculations was 3.6 μs (total unbiased and biased MD simulation being thus 7.8 μs).

Results and Discussion

G4 structure of the human telomeric DNA

The sequence of the G4 selected in this study is d[$AG_3(T_2AG_3)_3$], a 22-base sequence hereafter named **Tel22**. This human telomeric sequence can adopt different intramolecular G4 conformations depending on the aqueous solution conditions. In presence of Na^+ ions, this sequence forms an antiparallel "basket-type" structure, as elucidated by D. Patel et al. using NMR (PDB ID 143D, see Figure 1 d).[27a] This structure is characterized by a regular strand alternation and the presence of one diagonal and two lateral loops.[27a, 33] In presence of K^+, this DNA sequence presents a large polymorphism. A first structure was obtained by Neidle et al. using X-ray diffraction; it exhibits parallel strands and "double chain reversal" loops.[34] However, the relevance of this structure was much discussed since the crystallization conditions may have influenced the formation of this particular structure. Nowadays, it is considered that in presence of K^+, there is a mixture of parallel and anti-parallel G4 conformations, in a dynamic equilibrium between hybrid structures, as determined by NMR (PDB ID 2HY9, see Figure 1 b).[35] Those structures exhibit one "double chain reversal" and two parallel loops. The intramolecular G4 structures can be observed by CD experiments, as each conformation possesses a characteristic CD spectrum (see black lines in Figure 1 a,c). The CD spectra of **Tel22** in Na^+ medium shows a positive peak at 295 nm and an intense negative peak at 260 nm, characteristic of its anti-parallel conformation. In contrast, in a K^+ medium, the CD spectra of **Tel22** presents a positive maximum at 290 nm, a plateau at 265 nm, and a negative peak at 240 nm, characteristic of the hybrid structure.

Binding of Ru^{II} complexes to Human Telomeric G4-DNA

Buffered aqueous solutions of **Tel22** were mixed with each Ru complex (Scheme 1), and their binding was studied by UV/Vis absorption and CD spectroscopy with increasing concentrations of Ru complexes, expressed in molar equivalents per **Tel22** (at 0, 0.8, 1, 2, 3, 4, 5, 6, 7, 8, 9, 10 molar ratios, see Figure S1–S7 in the Supporting Information). The results are presented below for each type of G4 structure, that is, with solutions containing either Na^+ or K^+ ions. Given the difficulty to obtain enantiopure samples for each Ru complex under study, all the complexes experimentally studied here are in the form of a mixtures of optical isomers (i.e., Δ and Λ for mononuclear complexes), as for other studies on the binding of Ru complexes to G4s.[11c, e, 15] However, differences in terms of binding modes could occur for Δ or Λ isomers, as observed for the binding of Ru complexes to double-stranded DNA or other types of G4s.[12g–j]

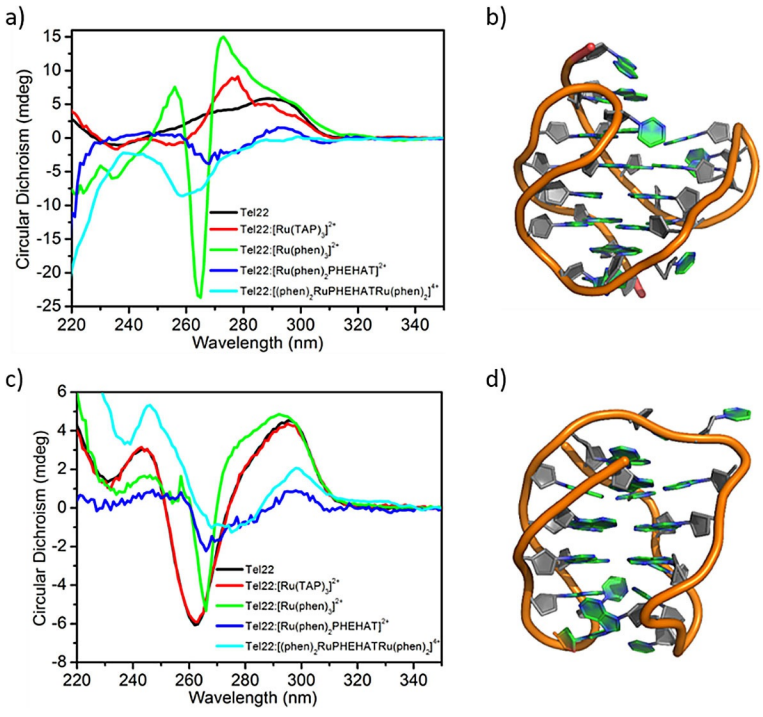

Figure 1. CD spectra of Tel22 recorded at 5 °C in a) TE buffer-K^+ and c) TE buffer-Na^+ (pH 7.4), in the presence of $[Ru(TAP)_3]^{2+}$, $[Ru(phen)_3]^{2+}$, $[Ru(phen)_2PHEHAT]^{2+}$ and $[(phen)_2RuPHEHATRu(phen)_2]^{4+}$ at 1:10 molar ratio in **Tel22**:Ru. Three-dimensional NMR structures of the b) mixed parallel/antiparallel structure (PDB ID: 2HY9, with K^+), and d) antiparallel basket G4 (PDB ID: 143D, with Na^+). Phosphate backbone and sugar moieties are depicted by the orange ribbon and filled gray rings, respectively. Bases are represented with filled rings. Images were rendered with PyMOL.

With K^+

Figure 1 a shows the CD spectra of the **Tel22**:Ru complex mixtures at 1:10 molar ratios in K^+ medium. In the case of binding to **$[Ru(TAP)_3]^{2+}$**, the intensity of the peak around 293 nm, characteristic of the antiparallel G4 folding, decreases, which indicates that the antiparallel G4 is destabilized (Figure 1 a and Figure S2–S3 in the Supporting Information). Moreover, the presence of a new positive peak at around 275 nm, which increases with the concentration of **$[Ru(TAP)_3]^{2+}$** (Figure S2–S3) and the presence of a slightly negative band at around 236 nm could suggest a larger extent of parallel G4 conformations. The most substantial changes occurred when **$[Ru(phen)_3]^{2+}$** is mixed with **Tel22** (see green line in Figure 1 a). The negative band at 265 nm (characteristic of the antiparallel conformation) increased sharply, and a positive band appeared at around 272 nm. However, the presence of a slightly negative band at around 240 nm is more characteristic of the parallel form, suggesting that a mixture of antiparallel and parallel G4 conformations remain. Note that the changes in CD signals in the spectral range where the DNA absorbs could also arise from a preferential binding of one of the Ru complex enantiomers (Δ or Λ), since it shows strong absorption

in the 200–300 nm region. Interestingly, with **[Ru(phen)$_3$]$^{2+}$**, an induced CD (ICD) signal is observed in the region around 450–500 nm, where only the Ru complex absorbs (see Figure S4). The ICD signature may be indicative of the interaction mode with G4 or a preferential binding for one of the enantiomers Δ or Λ for these G4.[36,37] Remarkably, both ICD signals and CD signals in the spectral region of DNA persisted when the solution was heated over 60 °C, as shown by variable-temperature CD experiment (Figure S4). Regarding **Tel22**:**[Ru(phen)$_2$PHEHAT]$^{2+}$**, we observed a new positive peak at around 270 nm and two negative peaks at around 257 nm and 280 nm up to 1:7 molar ratio (Figure S2). Further addition of heteroleptic complex yields the diminishment of these new bands (Figure 1 a). For the binuclear Ru complex, **[(phen)$_2$RuPHEHATRu(phen)$_2$]$^{4+}$**, no spectral changes were observed up to 1:7 molar ratio (Figure S2), which suggests that the conformation of **Tel22** was maintained. Upon addition of more equivalents of the binuclear Ru complex (up to 10), a negative CD signal appeared at around 260 nm (Figure 1 a).

With Na$^+$

The same studies were performed in NaCl solutions (Figure 1 c), where **Tel22** adopts an anti-parallel G4 conformation (Figure 1 d). For CD spectra of **Tel22** with **[Ru(TAP)$_3$]$^{2+}$**, we did not observe any change compared to the CD spectra of pure **Tel22** (Figure 1 c and Figure S5–S6). In contrast, the addition of **[Ru(phen)$_3$]$^{2+}$** to **Tel22** shows significant changes in CD spectra: the characteristic CD signal at 260 nm is red-shifted (around 4 nm) and sharpened, whereas the positive peak at around 295 nm is broader. For mixtures of **Tel22** and **[Ru(phen)$_2$PHEHAT]$^{2+}$**, we observed a decrease of the negative CD signal at 260 nm and the positive one at 295 nm, while the positive CD signal at 240 nm disappeared completely at a 1:1 molar ratio (Figure S5–S6). Finally, the interactions between **Tel22** and the binuclear complex **[(phen)$_2$RuPHEHATRu(phen)$_2$]$^{4+}$** at 1:3 molar ratio did not show important changes in the positions and shape of the CD spectra. However, upon increasing the concentration of Ru complex in the mixture, there is a decrease in the intensities of the 260 nm and 295 nm CD bands, and an increase of the positive CD signal at 240 nm. For the four mixtures, we did not observe ICD signals in the range where the Ru complexes absorb (Figure S7), in contrast to **Tel22**:**[Ru(phen)$_3$]$^{2+}$** in solutions with potassium.

Stabilization of Human Telomeric G4-DNA by Ru complexes

To further characterize the molecular recognition of **Tel22** by Ru complexes, FRET melting assays were performed. The FRET melting assay allows us to evaluate the stabilization (related to the affinity) of G4 ligands by measuring, using fluorescence spectroscopy, the melting properties of a double-dye labeled oligonucleotide, which shows FRET between the two dyes only when the oligonucleotide is folded in the G4 conformation (see sketch Figure S8).[23,38] The oligonucleotide sequence was end-capped with a fluorescein dye (FAM) at 5′-end and a tetramethylrhodamine (TAMRA) at 3′-end: 5′-FAM-GGG(T$_2$AG$_3$)$_3$-TAMRA-3′ (**F21T**), which is a very similar sequence of **Tel22**,[9d,38] and mimics the human telomeric repeat, allowing an intramolecular folding into a G4.[23,39] This modified human telomeric sequence is widely studied in literature for assessing the stabilization of G4-DNA by ligands.[9b,23,38,40] A first heating/cooling cycle of pure **F21T** is carried out, and after that the studied Ru complex is added to the solution. A new heating cycle of this mixture allows the determination of the half-melting temperature ($T_{1/2}$) by following the emission of the donor dye (i.e., FAM), which increases when the G4 structure unfolds as a function of temperature.[23] Importantly, the half-melting temperature difference ($\Delta T_{1/2}$) between the pure oligonucleotide (**F21T**) and the same oligonucleotide bound to a ligand, gives us a quantitative analysis of the stabilization effect induced by the ligand, and also a semi-quantitative evaluation of ligand binding affinity.[9b,10c,41] Note that the values reported here represent average values for the binding affinities of the optical isomers for each Ru complex (i.e., mixtures of Δ and Λ for mononuclear complexes, and $\Delta\Delta$, $\Lambda\Lambda$, $\Lambda\Delta$ for the binuclear complex). The FRET melting assays, as expressed by following the normalized FAM emission of **F21T** at different molar ratios in Tel22:Ru complex (1:3 and 1:10) in either Na^+ or K^+ environment, show that homoleptic **[Ru(TAP)$_3$]$^{2+}$** and **[Ru(phen)$_3$]$^{2+}$** complexes do not stabilize the G4 conformation: the $\Delta T_{1/2}$ values of **F21T**-**[Ru(TAP)$_3$]$^{2+}$** complex and **F21T**-**[Ru(phen)$_3$]$^{2+}$** complex are around 0–1 °C (Table 1, Figure 2, and Figures S9–S10). Interestingly, the two heteroleptic ligands, **[Ru(phen)$_2$PHEHAT]$^{2+}$** and **[(phen)$_2$RuPHEHATRu(phen)$_2$]$^{4+}$**, show a large increase of the $\Delta T_{1/2}$ (i.e., stabilization of the complex with respect to the **F21T** alone), ranging from a minimum $\Delta T_{1/2}$ of 13 °C to a maximum of 27 °C at 1:3 molar ratios. This stabilization was observed also when higher concentrations of complexes (1:10 molar ratio) were used both in Na^+ and K^+

Table 1. Half melting temperatures $T_{1/2}$ and half melting temperature differences $\Delta T_{1/2}$ (in °C) from FRET melting assays for each Ru complex, at various molar ratios in **F21T**:Ru. $T_{1/2}$ of pure **F21T** is 46 °C in solutions containing Na^+, and 51 °C in solutions containing K^+.

Complex	with Na^+				with K^+			
	1:3 **F21T**:Ru		1:10 **F21T**:Ru		1:3 **F21T**:Ru		1:10 **F21T**:Ru	
	$T_{1/2}$	$\Delta T_{1/2}$	$T_{1/2}$	$\Delta T_{1/2}$	$T_{1/2}$	$\Delta T_{1/2}$	$T_{1/2}$	$\Delta T_{1/2}$
[Ru(TAP)$_3$]$^{2+}$	46	0	46	0	56	5	51	0
[Ru(phen)$_3$]$^{2+}$	47	1	47	1	52	1	53	2
[Ru(phen)$_2$PHEHAT]$^{2+}$	68	22	64	18	78	27	82	31
[(phen)$_2$Ru PHEHATRu(phen)$_2$]$^{4+}$	67	21	72	26	64	13	76	25

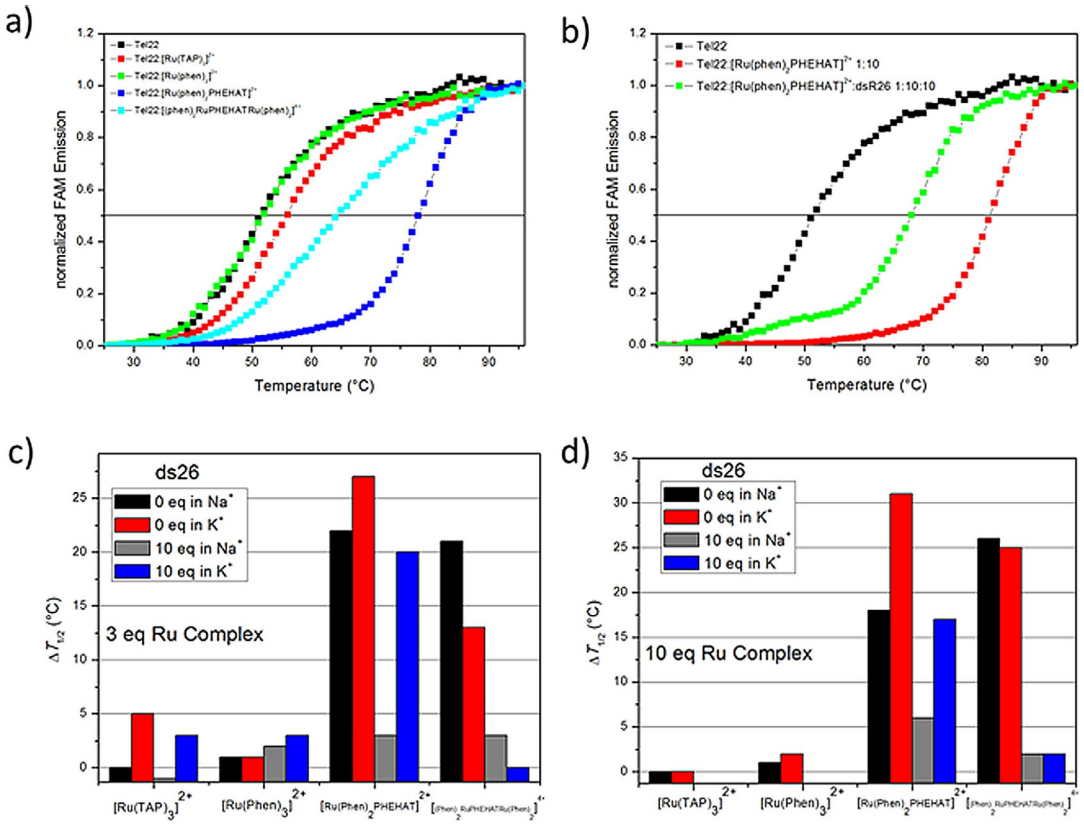

Figure 2. Up: Melting curves of 200 nM **F21T** in K^+ conditions in the presence of a) 1 μM Ru complexes and b) 3 μM $[Ru(phen)_2PHEHAT]^{2+}$-**F21T** complex without and with the presence of 10 molar equiv of competitor double-stranded DNA (ds26). The curves correspond to normalized FAM fluorescence. Bottom: Quantitative analysis of the competition experiments, with melting temperature differences for each type of Ru complex at c) 1 μM and at d) 3 μM without and with the presence of the competitor ds26 in Na^+ conditions (black and grey bars, respectively) and in K^+ conditions (red and blue bars, respectively). The measurements were performed using a 10 mM lithium cacodylate buffer (pH 7.2) with 10 mM NaCl, and using 10 mM lithium cacodylate buffer (pH 7.2) with 10 mM KCl and with 90 mM LiCl for Na^+ and K^+, respectively.

solutions. For **$[Ru(phen)_2PHEHAT]^{2+}$**, $\Delta T_{1/2}$ is higher in solutions containing K^+ than with Na^+, suggesting that this complex stabilizes more strongly the mixed hybrid conformation than the antiparallel one ($\Delta T_{1/2}$ of 27 °C in K^+ vs. 22 °C in Na^+ at 3 equiv). In contrast, **$[(phen)_2RuPHEHATRu(phen)_2]^{4+}$** stabilizes more strongly the antiparallel form than the hybrid conformations of human telomeric G4 ($\Delta T_{1/2}$ of 13 °C in K^+ vs. 21 °C in Na^+ at 3 equiv.). Globally, both heteroleptic complexes studied here could be considered as very good G4-ligands. For the sake of comparison, macrocyclic hexaoxazoles from Nagasawa et al. possess $\Delta T_{1/2}$ values close to 18 °C and 6 °C for symmetrical and unsymmetrical macrocyclic hexaoxazoles, respectively.[9c] Other organometallic compounds such as Pt-ttpy, Pt-ctpy, Cu-ttpy and Cu-ctpy (ttpy = 4′-*p*-tolyl-[2,2′;6′,2″] terpyridine; ctpy = 4′-ethynyl-2,2′:6′,2″-terpyridine) showed a $\Delta T_{1/2}$ of around 15 °C.[7a,42] Ru complexes such as $Ru[(bpy)_2(bqdppz)]^{2+}$ (bqdppz = benzo[*j*]quinoxalino[2,3-*h*]dipyrido[3,2-*a*:2′,3′-*c*]-phenazine)) reported by Chao et al. show a $\Delta T_{1/2}$ of 5 °C and 8 °C after the addition of 1 μM and 3 μM of complex, respectively, in solutions with Na^+; and 7 °C and 22 °C in K^+ solutions, respectively.[43] $[Ru(phen)_2dpq\text{-}df]^{2+}$ and $[Ru(bpy)_2dpq\text{-}df]^{2+}$ (dpq-df = dipyrido (3,2-*a*:2′,3′-*c*) quinoxaline-difuran) from Yao et al. were considered as excellent stabilizers of DNA G4s in K^+ solutions with $\Delta T_{1/2}$ of 14 °C and 13 °C, respectively.[44]

Selectivity of Ru complexes: G4-DNA versus dsDNA

Competition experiments were performed using FRET melting assays in order to assess the selectivity of the ligands for human telomeric G4 with respect to a double-stranded DNA. For that, we used a duplex oligonucleotide, of sequence 5′-CAATCGGATCGAATTCGATCCGATTG-3′ hybridized with its complementary sequence, hereafter called **ds26**. This double-stranded DNA was selected for its high melting temperature (T_m) around 70.5 °C, which is significantly higher than the T_m of **F21T** (around 50 °C).[23] For both homoleptic compounds **$[Ru(TAP)_3]^{2+}$** or **$[Ru(phen)_3]^{2+}$**, which do not show stabilization of **Tel22** (Table 1), the $T_{1/2}$ of **F21T**/Ru complex upon the addition of an excess of **ds26** remains similar than the $T_{1/2}$ obtained for the pure **F21T** both in Na^+ and K^+ solutions (Figure 2, Figures S11–S12 and Table S2). In contrast, the addition of 3 μM of the competitor **ds26** produces a strong destabilization of the **F21T:$[(phen)_2RuPHEHATRu(phen)_2]^{4+}$** complex ($\Delta T_{1/2}$ from ≈ +20 °C to ≈ +2 °C), indicating that this complex has no preference for either G4-DNA or dsDNA in the two solution conditions. It is important to highlight that for the other G4-ligand **$[Ru(phen)_2PHEHAT]^{2+}$**, the addition of the competitor yields a stabilization of around +18 °C for the **F21T:$[Ru(phen)_2$-PHEHAT$]^{2+}$** complex in K^+ solutions at a 1:10 molar ratio in

G4:Ru. This $\Delta T_{1/2}$ value is smaller to the one obtained for the complex in absence of a competitor (around +28 °C), but shows the preference of **[Ru(phen)$_2$PHEHAT]$^{2+}$** to bind to G4 rather than to double-stranded DNA (Figure 2). In contrast, the $\Delta T_{1/2}$ observed for the same ligand in Na^+ solutions ($\Delta T_{1/2} \approx +4$ °C) indicates the destabilization of the complex in the presence of the competitor **ds26**. Thus, these different $\Delta T_{1/2}$ observed in the two environments indicate that the ligand stabilizes more strongly the hybrid conformation over the antiparallel form of G4. The selectivity of **[Ru(phen)$_2$PHEHAT]$^{2+}$** towards G4 was confirmed even at higher concentration of **ds26** ($\approx$5 μM) in K^+ solutions (see Figure S13). The $\Delta T_{1/2}$ value obtained was nearly identical than that for the **F21T-[Ru(phen)$_2$PHEHAT]$^{2+}$** in the presence of $\approx$3 μM **ds26** competitor (+ 17 °C), indicating the weak affinity of **[Ru(phen)$_2$PHEHAT]$^{2+}$** to dsDNA compared to G4-DNA, even in excess of the double-stranded DNA competitor.

The interactions between the Ru complexes and the G4s were also evaluated by measuring the luminescence lifetimes of those complexes, which provides clues on the interactions between Ru complexes and DNA.[45] First, the luminescence lifetimes of the complexes were measured in absence of any DNA structure, see data presented in Table S3. For **[Ru(phen)$_2$PHEHAT]$^{2+}$** and **[(phen)$_2$RuPHEHATRu(phen)$_2$]$^{4+}$** complexes, no luminescence lifetime could have been measured in aqueous medium. Indeed, these complexes are known to present a "*light switch*" behaviour.[21] Luminescence lifetimes for these pure complexes measured in acetonitrile are presented in Table S3. First, the pure complexes in solution present mono-exponential decay which is characteristic of pure species in solution. Secondly, the luminescence lifetimes were measured in presence of human telomeric **Tel22** sequence in Na^+ and K^+ aqueous solutions. All measurements were performed with a 1:10 **Tel22**:Ru complex ratio (in order to have enough luminescent species in solution), and the data obtained are gathered in Table 2.

For both **[Ru(TAP)$_3$]$^{2+}$** and **[Ru(phen)$_3$]$^{2+}$** in presence of **Tel22**, the fitting has been performed in a satisfying manner with mono-exponential decay. A unique luminescence lifetime has thus been determined for these two homoleptic complexes, regardless the aqueous medium nature. The luminescence lifetimes are very similar to the one measured with the complexes pure in solution (see Table 2 and Table S2). The weak interactions between these complexes and the **Tel22** sequence, as assessed by FRET experiments, combined to the fact that we used a 1:10 molar ratio (**Tel22**:Ru complex) in these experiments, give rise to a great amount of free complexes in solution. The measured luminescence lifetimes correspond most likely to the vast majority of complexes that do not interact with the **Tel22** sequence. However, CD spectra indicate there are interactions between **[Ru(phen)$_3$]$^{2+}$** and **Tel22**. This apparent discrepancy could be explained by the binding modes of **[Ru(phen)$_3$]$^{2+}$** to G4 and the G4 structural deformation upon binding, see below. In contrast, the luminescence lifetimes show that the **[Ru(phen)$_2$PHEHAT]$^{2+}$** and **[(phen)$_2$RuPHEHATRu(phen)$_2$]$^{4+}$** complexes interact strongly with the **Tel22** sequence, in agreement with the FRET experiments. Regardless the solution conditions, the luminescence decays were adjusted by bi-exponential functions: two luminescence lifetimes (τ_i) and the corresponding pre-exponential factors (% B_i) were determined. The luminescence decays for these complexes present two contributions: a short and a longer one, which indicate the ability of these complexes to probe two different environments and thus to present two types of binding modes. Since these two complexes are composed of a planar extended ligand (PHEHAT), it suggests that an intercalation takes place in the binding, or at least partial intercalation. Furthermore, a relatively long contribution to the lifetime is observed which means that the complex is strongly protected by its environment. The (partial) intercalation of these complexes in the loops at the extremity of the G4 structure could correspond to the longer contribution of the luminescence lifetime (see below).

In solutions with K^+, the **[Ru(phen)$_2$PHEHAT]$^{2+}$** complex presents a contribution of 167 ns (86%), close to the lifetime value for this complex alone in acetonitrile, and a second contribution of 2 ns (14%). This complex clearly presents two binding modes with the hybrid G4 conformation of the **Tel22** sequence. In Na^+ medium, where the G4 antiparallel structure is favoured, **[Ru(phen)$_2$PHEHAT]$^{2+}$** shows a contribution of 44 ns (83%) and a second one of 2 ns (17%). The binding mode where the complex is less protected (for which the lifetime is the shortest) is present in similar proportions, regardless the alkali ion (K^+or Na^+) in the solution. Regarding the longest contribution, the lifetime value decreases when changing from K^+ to Na^+ media. Based on previously established assumptions, this could mean that the **[Ru(phen)$_2$PHEHAT]$^{2+}$** complex interacts more strongly with the hybrid structure formed in K^+ medium than with the anti-parallel structure formed in Na^+ medium, which is in fair agreement with the results obtained by FRET analysis.

The binuclear **[(phen)$_2$RuPHEHATRu(phen)$_2$]$^{4+}$** complex presents, in K^+ medium, a first contribution of 58 ns (77%) and a second one of 9 ns (23%). This complex presents also

Table 2. Luminescence lifetimes of the four complexes in presence of **Tel22** sequence (1:10 molar ratio in **Tel22**:Ru molar ratio) in TE buffer + 100 mM KCl (left) or NaCl (right).

Complex	K^+					Na^+				
	τ_1 [ns]	[% B_1]	τ_2 [ns]	[% B_2]	τ_m [ns]	τ_1 [ns]	[% B_1]	τ_2 [ns]	[% B_2]	τ_m [ns]
$[Ru(TAP)_3]^{2+}$	184	100	–	–	184	166	100	–	–	166
$[Ru(phen)_3]^{2+}$	461	100	–	–	461	455	100	-	–	455
$[Ru(phen)_2PHEHAT]^{2+}$	2	14	167	86	15	2	17	44	83	10
$[(phen)_2RuPHEHATRu(phen)_2]^{4+}$	9	23	58	77	26	8	5	64	95	49

two interaction modes with the hybrid conformation of **Tel22**. In Na^+ medium, the first contribution corresponds to 65 ns (95%) while the second one is 8 ns (5%). In this case, the longest contribution evolves from 77% (with the hybrid conformation) to 95% (with the antiparallel conformation). So, it seems that the antiparallel structure, presenting two lateral loops and a diagonal one, possesses a more favourable geometry for the (partial) intercalation of **$[(phen)_2$-RuPHEHATRu$(phen)_2]^{4+}$**.

The luminescence lifetimes were measured in presence of the competitor **ds26** in Na^+ and K^+ aqueous solution. All measurements were performed with a **ds26**:Ru molar ratio of 1:10 to have enough luminescent species in solution and the data obtained are gathered in Table 3.

For the homoleptic **$[Ru(TAP)_3]^{2+}$** and **$[Ru(phen)_3]^{2+}$** complexes, the fitting has been performed in a satisfying manner with mono-exponential decay. A unique luminescence lifetime has thus been determined for these two homoleptic complexes, regardless of the aqueous medium nature. Similar to previous measurements with **Tel22**, the luminescence lifetime is close to the one measured with the pure complexes, suggesting that with the double stranded DNA, at such a high salt concentration, these two complexes are mainly free in solution. In contrast, for **$[Ru(phen)_2PHEHAT]^{2+}$** and **$[(phen)_2$-RuPHEHATRu$(phen)_2]^{4+}$** complexes, luminescence decays were adjusted by bi-exponential functions regardless the alkali ion in the solution. It could also be concluded that the interaction of these complexes with **ds26** corresponds to two modes of interaction which could be the same as described before, namely a (partial) intercalation and an interaction in the grooves. **$[Ru(phen)_2PHEHAT]^{2+}$** shows two contributions of 66 ns (80%) and 19 ns (20%) in K^+ medium, whereas in Na^+ those contributions correspond to 250 ns (94%) and 3 ns (6%), respectively. Considering the previous assumptions about the interaction geometries, in Na^+ medium, it seems that the (partial) intercalation of the extended planar ligand is favoured. The second mode of interaction, which could be an interaction in the DNA groove, seems to be slightly more favoured in K^+ medium. For **$[(phen)_2RuPHEHATRu(phen)_2]^{4+}$**, two contributions are observed: 99 ns (83%) and 27 ns (17%) in K^+ medium, and 90 ns (86%) and 2 ns (14%) in Na^+. Once again, the interaction in the DNA groove is more favoured in K^+ medium as observed with **$[Ru(phen)_2PHEHAT]^{2+}$**. The importance of the two modes of interaction appears to be dependent on the nature of the salt used. This could be explained by differences of the double helix structure in function of the salt nature and concentration as described in the literature.[46] However, the nature and the concentration of alkali ion present in solution seem to have less influence on the intercalation binding mode. Comparing the results obtained with **Tel22** and **ds26** in K^+ medium for the **$[Ru(phen)_2PHEHAT]^{2+}$** or **$[(phen)_2RuPHEHATRu(phen)_2]^{4+}$** complexes, it seems that a binding mode in the DNA grooves (intramolecular grooves in G4-DNA or minor-groove in dsDNA) is likely.

Molecular modelling: binding modes of G4:Ru complexes

MD simulations were carried out to provide molecular insights about the G4:Ru-complex binding modes, focusing on the interactions between G4 and either **$[Ru(phen)_3]^{2+}$** or **$[Ru(phen)_2PHEHAT]^{2+}$**. These two ligands were selected because of their large difference in the stabilization of G4 (see Table 1). Note that only Δ isomers of these Ru complexes were considered for assessing the binding to G4s (1:1 ratio in G4:Ru complexes), for the sake of computational cost. For the binding of **$[Ru(phen)_3]^{2+}$**, both hybrid and antiparallel structures of human telomeric G4 structures were considered as this complex does not show any difference in the stabilization of G4 in solution with K^+ or Na^+. MD simulations were performed over a 300 ns timescale, allowing a proper sampling of (i) the motion of the Ru complex with respect to G4, and (ii) the structural modification of G4 upon Ru complex binding (see root-mean square deviation over MD simulation, Figure S14). The G-quartets of both hybrid and antiparallel G4 structures are referred to as *top*, *mid* and *bottom*, considering that the first guanine residue belong to the *top* quartet. The guanine bases in each quartet are referred to as α-, β-, γ- and δ-guanines, to ease the description of structural findings by MD simulations (see Figure S15).

Binding modes of $[Ru(phen)_3]^{2+}$ with G4 structures

From the four starting conformations of **$[Ru(phen)_3]^{2+}$** in interaction with the hybrid G4 structure, MD runs reveal two main binding modes, namely bottom and the top/minor groove mode (see Figure 3a, Table S4 and Figures S16–S17 in the Supporting Information). As the G-quartets of the hybrid G4 structures are surrounded by the loops, the direct interaction between **$[Ru(phen)_3]^{2+}$** and G-quartet requires ligand intercalation between the phosphate backbone strands. In the bottom binding mode, **$[Ru(phen)_3]^{2+}$** intercalates below the bottom quartet, see Figure 3a. In these modes, **$[Ru(phen)_3]^{2+}$** interacts either directly with the bottom G-quartet guanine residues (namely dG_6 and dG_{24}) or with the dA_{15} and dA_{26} residues, a

Table 3. Luminescence lifetimes of the four Ru complexes in presence of double stranded DNA ds26 in TE buffer + 100 mM KCl (left) or NaCl (right).

Complex	K^+					Na^+				
	τ_1 [ns]	[% B_1]	τ_2 [ns]	[% B_2]	τ_m [ns]	τ_1 [ns]	[% B_1]	τ_2 [ns]	[% B_2]	τ_m [ns]
$[Ru(TAP)_3]^{2+}$	196	100	–	–	196	152	100	–	–	152
$[Ru(phen)_3]^{2+}$	489	100	–	–	489	399	100	–	–	399
$[Ru(phen)_2PHEHAT]^{2+}$	19	20	66	80	44	3	6	250	94	37
$[(phen)_2RuPHEHATRu(phen)_2]^{4+}$	27	17	99	83	67	2	14	90	86	14

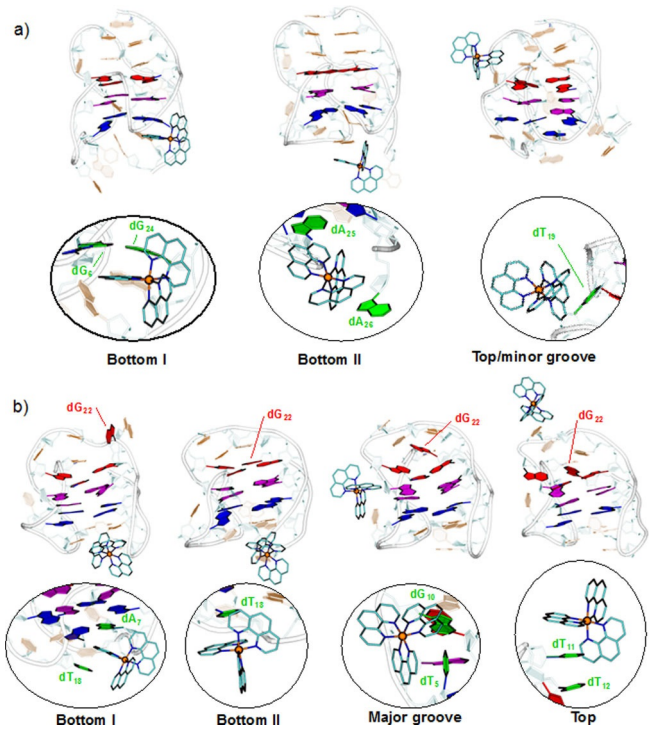

Figure 3. Representative snapshots of the main binding modes of Δ-$[Ru(phen)_3]^{2+}$ with a) hybrid and b) antiparallel G4 structures from MD simulations. Guanine moieties Top, Mid and Bottom quartets are depicted in red, purple and blue, respectively. Other nucleic acids are coloured in orange. Hydrogen atoms are omitted for sake of clarity. Residues involved in the binding with $[Ru(phen)_3]^{2+}$ are depicted in green.

binding mode often referred to as *end-stacking* mode in the literature. In the top/minor groove mode, **$[Ru(phen)_3]^{2+}$** intercalates on the top side of the minor groove, interacting with sidechain nucleic residues (e.g., dT_{19}). In both conformations, **$[Ru(phen)_3]^{2+}$** is strongly anchored in close contact with the hybrid G4 structure, as shown by the narrow distribution of distances between **$[Ru(phen)_3]^{2+}$** and the guanine residues of importance (see Table S5 and Figure S22). These binding modes lead to structural deformations of **$[Ru(phen)_3]^{2+}$**, that could also explain the experimentally observed induced CD signals in the spectral range of the Ru complex (see Figure S4).

In the MD simulations of the antiparallel **Tel22** with **$[Ru(phen)_3]^{2+}$**, we observed three binding modes namely the bottom, the major groove and the top, see Figure 3b (and Figures S18–S19 in the Supporting Information). Interestingly, **$[Ru(phen)_3]^{2+}$** binds more superficially to antiparallel G4 than to hybrid G4, that is to say it does not intercalate as deeply in between the G4-phosphate backbone strands, leading to a lower structural deformation of **$[Ru(phen)_3]^{2+}$** than in the case of the hybrid (K^+) G4. This might explain why an induced CD signals was not experimentally observed for the **$[Ru(phen)_3]^{2+}$** complex in interaction with G4 in Na^+ solution. The bottom binding mode may be divided into two sub-binding modes in which one phenanthroline moiety of **$[Ru(phen)_3]^{2+}$** ligand interacts either with both dA_7 and dT_{18} residues in a sandwich-manner or only with dT_{18} (see Figure 3b left). MD simulations also reveal a major groove binding mode involving π-stacking interactions with dT_5 and dG_{10} as well as top-type binding mode in which the **$[Ru(phen)_3]^{2+}$** phenanthroline stacks on top of dT_{11}-dT_{12}.

It is worth mentioning that MD simulations reveal that the G4 also undergo conformational rearrangement upon **$[Ru(phen)_3]^{2+}$** binding. With the hybrid G4 (with K^+), a slight structural deformation compared to the initial G4 structure may occur for the bottom binding mode, in which **$[Ru(phen)_3]^{2+}$** interacts with dA_{26} without intercalating into the G4 structure. However, the inter-quartet distance varies only by at the most 0.4 Å with respect to the pure hybrid G4 structure (see Table S6). In contrast, for the antiparallel G4, larger conformational rearrangements can occur upon **$[Ru(phen)_3]^{2+}$** binding. For instance, the top/mid inter-quartet distance increases or decreases by some 1.0 Å, from 5.0±0.2 Å for the pure G4, to 6.0±0.2 Å for the bottom binding mode, and 4.0±0.4 Å for major-groove binding (see Table S6). We note a high flexibility of the γ-guanine residue in the Top quartet of antiparallel G4 (namely dG_{22}), which can flip outside the top G-quartet plane. Except for the top binding, the presence of **$[Ru(phen)_3]^{2+}$** somewhat increases the flipping of dG_{22} (see Figure 3b), leading to the formation of a guanine-triplex arrangement (involving dG_2, dG_{10} and dG_{14}) instead of a G-quartet at the top of G4 (as pictured by the distance between dG_{22} and the Tel22 core in Figure S23 in the Supporting Information). Altogether, these binding modes in the loops and the structural deformation of G4 agree with both the interaction between **$[Ru(phen)_3]^{2+}$** and G4 observed by CD spectroscopy and the very weak stabilization of G4 upon **$[Ru(phen)_3]^{2+}$** observed by melting temperature experiments. Again, differences in terms binding modes could occur for Δ or Λ isomers, as observed for the binding of other Ru complexes to G4s,[12i–j] an issue that will be explored in our future modeling studies.

Binding modes of $[Ru(phen)_2PHEHAT]^{2+}$ with hybrid G4

From the four starting conformations of **$[Ru(phen)_2PHEHAT]^{2+}$** in interaction with hybrid G4 structure, MD simulations also reveal two similar main binding modes with respect to **$[Ru(phen)_3]^{2+}$**, namely bottom and top modes, which is in agreement with the luminescence lifetime experiments (see Figure 4, Table S4 and Figures. S18–S19 in the Supporting Information). In the Bottom binding modes, **$[Ru(phen)_2PHEHAT]^{2+}$** can either intercalate between the phosphate backbone strand if only phenanthroline ligands interact with the nucleic acid residues (namely dA_{26} and dG_6), or interact with dA_{26}, dA_{25} and dA_{15} following an end-stacking mode. Similarly to **$[Ru(phen)_3]^{2+}$**, Bottom binding modes do not significantly modify inter-quartet distances with respect to pure hybrid G4 structure (maximum deviations of 0.2 Å are observed). The top binding mode differs from the **$[Ru(phen)_3]^{2+}$** top/minor mode by intercalation into the G4 major groove owing to the bulkier structure of **$[Ru(phen)_2PHEHAT]^{2+}$**. This allows π-stacking interactions with three off-quartet residues (namely, dA_9, dA_1 and dA_2). Interestingly, the top binding mode leads to a significant deformation of one quartet. Although the top/mid inter-quartet distance is not strongly modified by the

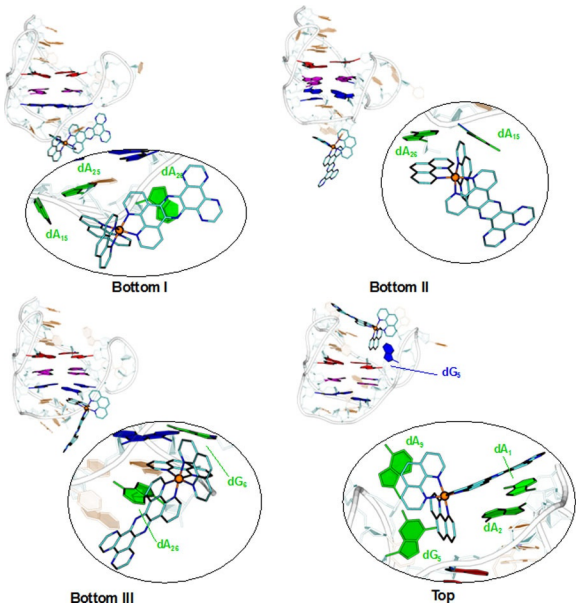

Figure 4. Representative snapshots of the main binding modes of Δ- [Ru(phen)$_2$PHEHAT]$^{2+}$ with hybrid G4 from MD simulations. Guanine moieties Top, Mid and Bottom quartets are depicted in red, purple and blue, respectively. Other nucleic acids are coloured in orange. Hydrogen atoms are omitted for sake of clarity. Residues of importance involved in the binding are depicted in green.

presence of **[Ru(phen)$_2$PHEHAT]$^{2+}$**, the bottom quartet is strongly modified owing to the flipping of its α-guanine (namely dG_6, see Figure 4 and Table S4). Such an event might allow to stabilize π-stacking interactions between the mid and top quartets resulting in π-stacked triplex-quartet-quartet G4 structure. This partial intercalation is in line with the longer contribution to the luminescence lifetime of **[Ru(phen)$_2$PHEHAT]$^{2+}$** in presence of hybrid G4, see above.

Binding energies of G4:Ru complexes

To assess the preferential binding modes over the conformations obtained by MD, pulling PMF calculations and corresponding binding free energies $\Delta\Delta G_{SMD}$ were calculated from SMD simulations as well as total intermolecular interactions energies between the Ru complex and G4. The SMD reaction coordinate x was defined as the distance from the equilibrium distance between **[Ru(phen)$_3$]$^{2+}$** and the interacting nucleic acids obtained from equilibrium MD simulation (x_{eq}) over the pulling, that is, ranging from x_{eq} to $x_{eq}+30$ Å (see the free energy profiles in Figure S24). The stronger the interaction between the Ru-based complex and the G4-structure, the larger the PMF, and the larger the unbinding free energy. The interaction energies and unbinding free energies are reported in Table 4 for complexes between the Ru compounds **[Ru(phen)$_3$]$^{2+}$** and **[Ru(phen)$_2$PHEHAT]^2** and hybrid G4. This comparison is relevant as, in K^+ solutions (hybrid form), we observed the largest difference in G4 stabilization between **[Ru(phen)$_3$]$^{2+}$** and **[Ru(phen)$_2$PHEHAT]^2** ($\Delta T_{1/2}$ of 1 °C and 27 °C for **[Ru(phen)$_3$]$^{2+}$** and **[Ru(phen)$_2$PHEHAT]^2** at 1:3 equiv., respectively, see Table 1). For the binding of **[Ru(phen)$_3$]$^{2+}$** to hybrid G4, the preferential binding (higher ΔG_{unbind}) is bottom > top/minor groove. This bottom binding mode differs from the binding modes of Ni^{II}-porphyrin compounds to human telomeric DNA G4,[9d] where complexes adopt either planar or saddle conformations. In contrast, homoleptic Ru complexes are more rigid and present an octahedral coordination. Likewise, **[Ru(phen)$_2$PHEHAT]$^{2+}$** preferentially binds to hybrid G4 by means of a bottom mode rather than a top mode. The top or groove-binding modes are less favourable with respect to the bottom binding mode, due to the larger steric hindrance between **[Ru(phen)$_2$PHEHAT]$^{2+}$** and the loops (G4 phosphate backbone) on top compared to bottom. The estimates of the van der Waals energy (E_{vdW} in Table 4) show their larger contribution to the total non-covalent energy of interaction (E_{nc} in Table 4) in the bottom mode for the two complexes. It must be stressed that **[Ru(phen)$_2$PHEHAT]$^{2+}$** in comparison with **[Ru(phen)$_3$]$^{2+}$** binds more strongly to the hybrid G4 (i.e., larger ΔG_{unbind}), regardless the type of binding mode. This is attributed to stronger π-stacking interactions between the PHEHAT and the adenine bases of the G4 loops (see zooms in Figure 4), which is reflected by the large van der Waals contributions to the total non-covalent energy of interaction (see Table 4). The differences in unbinding free energies for the two complexes are in line with the differences in stabilization of G4, estimated through melting temperature experiments reported in Table 1.

Conclusions

We have reported the molecular recognition properties of a series of Ru complexes by DNA G4s formed by a human telomeric sequence, in various solution conditions (i.e., with K^+ or Na^+). The two homoleptic complexes **[Ru(TAP)$_3$]$^{2+}$** and **[Ru(phen)$_3$]$^{2+}$** interact weakly with G4, as probed by melting temperature and luminescence lifetime measurements. However, the binding between **[Ru(phen)$_3$]$^{2+}$** and G4 leads to in-

Table 4. Binding energies of 1:1 Ru:G4 complexes from 100 ns MD and SMD simulations. Non-covalent binding energies (E_{nc}, in kcal mol^{-1}) are decomposed in coulombic and van der Waals (E_{coul} and E_{vdW}, in kcal mol^{-1}). The unbinding free energies at $x=30$ Å were computed from SMD-PMF calculations (ΔG_{unbind}, in kcal mol^{-1}).

		E_{coul}	E_{vdW}	E_{nc}	ΔG_{unbind}
Δ-[Ru(phen)$_3$]$^{2+}$	Bottom	−101.3 ± 10.1	−39.3 ± 3.2	−140.6 ± 12.1	10.1 ± 1.0
	Top/minor groove	−110.7 ± 6.1	−30.9 ± 1.9	−141.6 ± 6.7	7.1 ± 0.7
Δ-[Ru(phen)$_2$PHEHAT]$^{2+}$	Bottom	−113.9 ± 8.6	−66.2 ± 3.9	−180.1 ± 10.4	18.7 ± 1.7
	Top	−85.9 ± 21.4	−55.9 ± 8.0	−141.8 ± 28.6	11.5 ± 2.0

duced CD signals in the spectral region where the Ru complex absorbs as well as large changes in the CD signals of the G4 DNA in K^+ solutions. MD simulations performed for **[Ru(phen)$_3$]$^{2+}$** show that the complex may interact through distinct binding modes to G4, referred to as top, bottom, and groove modes, and it may deform the structure of the G4, especially for the hybrid G4 structure in K^+. In contrast, the two heteroleptic Ru complexes, namely **[Ru(phen)$_2$PHEHAT]$^{2+}$** and **[(phen)$_2$RuPHEHATRu(phen)$_2$]$^{4+}$**, show an important stabilization of G4 ($\Delta T_{1/2}$ from 13 °C to 31 °C). **[Ru(phen)$_2$PHEHAT]$^{2+}$** exhibits a large selectivity towards G4 versus double-stranded DNA, as determined by competition experiments. This is rationalized by molecular modelling of the binding of the **[Ru(phen)$_2$PHEHAT]$^{2+}$** complex to hybrid G4, showing that interactions with the loops as well as the π-type interactions between adenine bases and **PHEHAT** strongly stabilize the partial intercalation of the complex in G4 (in the bottom binding mode), with a larger binding free energy than for **[Ru(phen)$_3$]$^{2+}$**. Together with their "light switch" behaviour, the two Ru heteroleptic ligands are therefore attractive in view of their recognition properties towards G4, which could be exploited for binding to other G4s, such as those formed in oncogene promoters of therapeutic potential against cancers. Our future works will focus on the origin of the ICD signals observed for the binding of **[Ru(phen)$_3$]$^{2+}$** to human telomeric DNA G4s, as well as the possible differences of G4 binding modes between enantiomers of Ru complexes.

Acknowledgements

This work was supported by the Fonds de la Recherche Scientifique-FNRS (Belgium) under the grants n°1.B333.15F (CHIRNATES), F.4532.16 (MIS-SHERPA), 2.4530.12, 2.4615.11, UN02715F and CDR J.0022.18. This research was supported by the Interuniversity Attraction Poles Programme (PAI 7/05) initiated by the Belgian Science Policy Office. J.R.-M. and M.F. are FNRS post-doctoral researchers and M.S. is Maître de Recherches FNRS. S.K. thanks the "Fonds pour la Formation à la Recherche dans l'Industrie et dans l'Agriculture" (FRIA) for funding. F.D.M. and P.T. thank Institut National de la Santé et de la Recherche Médicale (INSERM) and Nouvelle Aquitaine Region for funding and CALI for computational resources. F.D.M. and M.L. are grateful to Swedish e-Research Council (SeRC) and National Supercomputing Center (NSC) for computational resources. P.T. thanks the Czech Science Foundation (P208/12/G016) and National Program of Sustainability I from the Ministry-of-Youth, Education and Sports of the Czech Republic (LO1305). M.S. thanks Dr. Lionel Marcélis for helpful discussions.

Conflict of interest

The authors declare no conflict of interest.

Keywords: DNA recognition · G-quadruplexes · light switches · ruthenium complexes

[1] M. Gellert, M. N. Lipsett, D. R. Davies, *Proc. Natl. Acad. Sci. U. S. A.* **1962**, *48*, 2013 – 2018.

[2] a) G. Biffi, D. Tannahill, J. McCafferty, S. Balasubramanian, *Nat. Chem.* **2013**, *5*, 182 – 186; b) N. Maizels, L. T. Gray, *PLoS Genet.* **2013**, *9*, e1003468; c) B. Maji, S. Bhattacharya, *Chem. Commun.* **2014**, *50*, 6422 – 6438; d) Y. Wu, R. M. Brosh, *FEBS J.* **2010**, *277*, 3470 – 3488; e) T. Simonsson, *Biol. Chem.* **2001**, *382*, 621 – 628; f) N. Maizels, *Nat. Struct. Biol.* **2006**, *13*, 1055 – 1059.

[3] M. T. Teixeira, E. Gilson, *Chromosome Res.* **2005**, *13*, 535 – 548.

[4] a) C. Wei, C. M. Price, *CMLS, Cell. Mol. Life Sci.* **2003**, *60*, 2283 – 2294; b) W. E. Wright, V. M. Tesmer, K. E. Huffman, S. D. Levene, J. W. Shay, *Genes Dev.* **1997**, *11*, 2801 – 2809.

[5] a) S. M. Bailey, J. P. Murnane, *Nucleic Acids Res.* **2006**, *34*, 2408 – 2417; b) R. J. O'Sullivan, J. Karlseder, *Nat. Rev. Mol. Cell Biol.* **2010**, *11*, 171 – 181.

[6] a) S. Balasubramanian, S. Neidle, *Curr. Opin. Chem. Biol.* **2009**, *13*, 345 – 353; b) M. Bončina, J. Lah, I. Prislan, G. Vesnaver, *J. Am. Chem. Soc.* **2012**, *134*, 9657 – 9663; c) H. Yaku, T. Fujimoto, T. Murashima, D. Miyoshi, N. Sugimoto, *Chem. Commun.* **2012**, *48*, 6203 – 6216.

[7] a) D. Monchaud, M. P. Teulade-Fichou, *Org. Biomol. Chem.* **2008**, *6*, 627 – 636; b) H. Han, L. H. Hurley, *Trends Pharmacol. Sci.* **2000**, *21*, 136 – 142; c) T. M. Ou, Y. J. Lu, J. H. Tan, Z. S. Huang, K. Y. Wong, L. Q. Gu, *ChemMedChem* **2008**, *3*, 690 – 713; d) S. Neidle, *Curr. Opin. Struct. Biol.* **2009**, *19*, 239 – 250; e) D. Yang, K. Okamoto, *Future Med. Chem.* **2010**, *2*, 619 – 646; f) S. Neidle, *Nat. Rev. Chem.* **2017**, *1*, 0041.

[8] a) D. M. Răsădean, B. Sheng, J. Dash, G. D. Pantos, *Chem. Eur. J.* **2017**, *23*, 8491 – 8499; b) K. Padmapriya, R. Barthwal, *Biophys. Chem.* **2016**, *219*, 49 – 58.

[9] a) A. De Cian, E. DeLemos, J.-L. Mergny, M.-P. Teulade-Fichou, D. Monchaud, *J. Am. Chem. Soc.* **2007**, *129*, 1856 – 1857; b) D. Monchaud, A. Granzhan, N. Saettel, A. Guédin, J.-L. Mergny, M.-P. Teulade-Fichou, *J. Nucleic Acids* **2010**, *2010*, 525862; c) M. Sakuma, Y. Ma, Y. Tsushima, K. Iida, T. Hirokawa, K. Nagasawa, *Org. Biomol. Chem.* **2016**, *14*, 5109 – 5116; d) J. Rubio-Magnieto, F. Di Meo, M. Lo, C. Delcourt, S. Clément, P. Norman, S. Richeter, M. Linares, M. Surin, *Org. Biomol. Chem.* **2015**, *13*, 2453 – 2463.

[10] a) S. N. Georgiades, N. H. Abd Karim, K. Suntharalingam, R. Vilar, *Angew. Chem. Int. Ed.* **2010**, *49*, 4020 – 4034; *Angew. Chem.* **2010**, *122*, 4114 – 4128; b) J. Zhang, F. Zhang, H. Li, C. Liu, J. Xia, L. Ma, W. Chu, Z. Zhang, C. Chen, S. Li, S. Wang, *Curr. Med. Chem.* **2012**, *19*, 2957 – 2975; c) A. Arola, R. Vilar, *Curr. Top. Med. Chem.* **2008**, *8*, 1405 – 1415; d) T. Vy Thi Le, S. Han, J. Chae, H. J. Park, *Curr. Pharm. Des.* **2012**, *18*, 1948 – 1972.

[11] a) Y. L. Jiang, Z. P. Liu, *Mini. Rev. Med. Chem.* **2010**, *10*, 726 – 736; b) Q. Cao, Y. Li, E. Freisinger, P. Z. Qin, R. K. O. Sigel, Z.-W. Mao, *Inorg. Chem. Front.* **2017**, *4*, 10 – 32; c) G. Piraux, L. Bar, M. Abraham, T. Lavergne, H. Jamet, J. Dejeu, L. Marcélis, E. Defrancq, B. Elias, *Chem. Eur. J.* **2017**, *23*, 11872 – 11880; d) E. Wachter, D. Moya, S. Parkin, E. C. Glazer, *Chem. Eur. J.* **2016**, *22*, 550 – 559; e) D. Saadallah, M. Bellakhal, S. Amor, J.-F. Lefebvre, M. Chavarot-Kerlidou, I. Baussanne, C. Moucheron, M. Demeunynck, D. Monchaud, *Chem. Eur. J.* **2017**, *23*, 4967 – 4972.

[12] a) M. J. Clarke, *Coord. Chem. Rev.* **2003**, *236*, 209 – 233; b) I. Kostova, *Curr. Med. Chem.* **2006**, *13*, 1085 – 1107; c) A. Levina, A. Mitra, P. A. Lay, *Metallomics* **2009**, *1*, 458 – 470; d) M. G. Mendoza-Ferri, C. G. Hartinger, M. A. Mendoza, M. Groessl, A. E. Egger, R. E. Eichinger, J. B. Mangrum, N. P. Farrell, M. Maruszak, P. J. Bednarski, F. Klein, M. A. Jakupec, A. A. Nazarov, K. Severin, B. K. Keppler, *J. Med. Chem.* **2009**, *52*, 916 – 925; e) A. N. Boynton, L. Marcélis, J. K. Barton, *J. Am. Chem. Soc.* **2016**, *138*, 5020 – 5023; f) L. Zeng, P. Gupta, Y. Chen, E. Wang, L. Ji, H. Chao, Z. S. Chen, *Chem. Soc. Rev.* **2017**, *46*, 5771 – 5804; g) J. Andersson, P. Lincoln, *J. Phys. Chem. B* **2011**, *115*, 14768 – 14775; h) J. P. Hall, D. Cook, S. Ruiz Morte, P. McIntyre, K. Buchner, H. Beer, D. J. Cardin, J. A. Brazier, G. Winter, J. M. Kelly, C. J. Cardin, *J. Am. Chem. Soc.* **2013**, *135*, 12652 – 12659; i) S. Shi, J.-H. Xu, X. Gao, H.-L. Huang, T.-M. Yao, *Chem. Eur. J.* **2015**, *21*, 11435 – 11445.

[13] a) R. M. Hartshorn, J. K. Barton, *J. Am. Chem. Soc.* **1992**, *114*, 5919 – 5925; b) A. E. Friedman, J. C. Chambron, J. P. Sauvage, N. J. Turro, J. K. Barton, *J. Am. Chem. Soc.* **1990**, *112*, 4960 – 4962; c) A. E. Friedman, C. V. Kumar, N. J. Turro, J. K. Barton, *Nucleic Acids Res.* **1991**, *19*, 5403 – 5408.

[14] S. Shi, X. Geng, J. Zhao, T. Yao, C. Wang, D. Yang, L. Zheng, L. Ji, *Biochimie* **2010**, *92*, 370 – 377.

[15] C. Rajput, R. Rutkaite, L. Swanson, I. Haq, J. A. Thomas, *Chem. Eur. J.* **2006**, *12*, 4611 – 4619.

[16] Z. Chen, K.-w. Zheng, Y.-h. Hao, Z. Tan, *J. Am. Chem. Soc.* **2009**, *131*, 10430 – 10438.
[17] T. Wilson, M. P. Williamson, J. A. Thomas, *Org. Biomol. Chem.* **2010**, *8*, 2617 – 2621.
[18] T. Wilson, P. J. Costa, V. Félix, M. P. Williamson, J. A. Thomas, *J. Med. Chem.* **2013**, *56*, 8674 – 8683.
[19] S. Rickling, L. Ghisdavu, F. Pierard, P. Gerbaux, M. Surin, P. Murat, E. Defrancq, C. Moucheron, A. Kirsch-De Mesmaeker, *Chem. Eur. J.* **2010**, *16*, 3951 – 3961.
[20] A. Kirsch-De Mesmaeker, R. Nasielski-Hinkens, D. Maetens, D. Pauwels, J. Nasielski, *Inorg. Chem.* **1984**, *23*, 377 – 379.
[21] C. Moucheron, A. Kirsch-De Mesmaeker, S. Choua, *Inorg. Chem.* **1997**, *36*, 584 – 592.
[22] J. Leveque, B. Elias, C. Moucheron, A. Kirsch-De Mesmaeker, *Inorg. Chem.* **2005**, *44*, 393 – 400.
[23] A. De Cian, L. Guittat, M. Kaiser, B. Saccà, S. Amrane, A. Bourdoncle, P. Alberti, M.-P. Teulade-Fichou, L. Lacroix, J.-L. Mergny, *Methods* **2007**, *42*, 183 – 195.
[24] J. Wang, R. M. Wolf, J. W. Caldwell, P. A. Kollman, D. A. Case, *J. Comput. Chem.* **2004**, *25*, 1157 – 1174.
[25] P. Brandt, T. Norrby, B. Åkermark, P.-O. Norrby, *Inorg. Chem.* **1998**, *37*, 4120 – 4127.
[26] M.-E. Moret, I. Tavernelli, U. Rothlisberger, *J. Phys. Chem. B* **2009**, *113*, 7737 – 7744.
[27] a) Y. Wang, D. J. Patel, *Structure* **1993**, *1*, 263 – 282; b) J. Dai, C. Punchihewa, A. Ambrus, D. Chen, R. A. Jones, D. Yang, *Nucleic Acids Res.* **2007**, *35*, 2440 – 2450.
[28] a) V. Hornak, R. Abel, A. Okur, B. Strockbine, A. Roitberg, C. Simmerling, *Proteins: Struct. Funct. Bioinf.* **2006**, *65*, 712 – 725; b) A. Pérez, F. J. Luque, M. Orozco, *J. Am. Chem. Soc.* **2007**, *129*, 14739 – 14745.
[29] D. J. Price, C. L. Brooks, *J. Chem. Phys.* **2004**, *121*, 10096 – 10103.
[30] D. R. Roe, T. E. Cheatham, *J. Chem. Theory Comput.* **2013**, *9*, 3084 – 3095.
[31] O. Perišić, H. Lu, *PLoS ONE* **2014**, *9*, e101810.
[32] a) S. Park, K. Schulten, *J. Chem. Phys.* **2004**, *120*, 5946 – 5961; b) S. Park, F. Khalili-Araghi, E. Tajkhorshid, K. Schulten, *J. Chem. Phys.* **2003**, *119*, 3559 – 3566.
[33] Y. Wang, D. J. Patel, *J. Mol. Biol.* **1993**, *234*, 1171 – 1183.
[34] G. N. Parkinson, M. P. H. Lee, S. Neidle, *Nature* **2002**, *417*, 876 – 880.
[35] a) K. N. Luu, A. T. Phan, V. Kuryavyi, L. Lacroix, D. J. Patel, *J. Am. Chem. Soc.* **2006**, *128*, 9963 – 9970; b) J. Dai, M. Carver, C. Punchihewa, R. A. Jones, D. Yang, *Nucleic Acids Res.* **2007**, *35*, 4927 – 4940; c) A. T. Phan, K. N. Luu, D. J. Patel, *Nucleic Acids Res.* **2006**, *34*, 5715 – 5719; d) J. Dai, M. Carver, D. Yang, *Biochimie* **2008**, *90*, 1172 – 1183; e) A. Ambrus, D. Chen, J. Dai, T. Bialis, R. A. Jones, D. Yang, *Nucleic Acids Res.* **2006**, *34*, 2723 – 2735; f) M. Bončina, J. Lah, I. Prislan, G. Vesnaver, *J. Am. Chem. Soc.* **2012**, *134*, 9657 – 9663; g) J. Dai, C. Punchihewa, A. Ambrus, D. Chen, R. A. Jones, D. Yang, *Nucleic Acids Res.* **2007**, *35*, 2440 – 2450; h) S. Shi, H.-L. Huang, X. Gao, J.-L. Yao, C.-Y. Lv, J. Zhao, W.-L. Sun, T.-M. Yao, L.-N. Ji, *J. Inorg. Biochem.* **2013**, *121*, 19 – 27.
[36] a) I. Lubitz, N. Borovok, A. Kotlyar, *Biochemistry* **2007**, *46*, 12925 – 12929; b) J. Pan, S. Zhang, *J. Biol. Inorg. Chem.* **2009**, *14*, 401 – 407.
[37] P. Zhao, J. Z. Lu, F. Y. Hong, B. H. Ou, F. D. Zhang, L. N. Ma, H. M. Guo, *Spectrochim. Acta Part A* **2013**, *108*, 1 – 7.
[38] D. Renčiuk, J. Zhou, L. Beaurepaire, A. Guédin, A. Bourdoncle, J.-L. Mergny, *Methods* **2012**, *57*, 122 – 128.
[39] a) J.-L. Mergny, J.-C. Maurizot, *ChemBioChem* **2001**, *2*, 124 – 132; b) B. Juskowiak, S. Takenaka in *Fluorescence Resonance Energy Transfer in the Studies of Guanine Quadruplexes* (Ed. V. V. Didenko), Humana Press, Totowa, NJ, **2006**, pp. 311 – 341.
[40] K. Duskova, S. Sierra, M.-S. Arias-Pérez, L. Gude, *Bioorg. Med. Chem.* **2016**, *24*, 33 – 41.
[41] P. A. Rachwal, K. R. Fox, *Methods* **2007**, *43*, 291 – 301.
[42] D. Monchaud, C. Allain, H. Bertrand, N. Smargiasso, F. Rosu, V. Gabelica, A. De Cian, J. L. Mergny, M. P. Teulade-Fichou, *Biochimie* **2008**, *90*, 1207 – 1223.
[43] G. L. Liao, X. Chen, L. N. Ji, H. Chao, *Chem. Commun.* **2012**, *48*, 10781 – 10783.
[44] X. H. Lu, S. Shi, J. L. Yao, X. Gao, H. L. Huang, T. M. Yao, *J. Inorg. Biochem.* **2014**, *140*, 64 – 71.
[45] a) A. J. McConnell, M. H. Lim, E. D. Olmon, H. Song, E. E. Dervan, J. K. Barton, *Inorg. Chem.* **2012**, *51*, 12511 – 12520; b) M. H. Lim, H. Song, E. D. Olmon, E. E. Dervan, J. K. Barton, *Inorg. Chem.* **2009**, *48*, 5392 – 5397; c) E. Largy, A. Granzhan, F. Hamon, D. Verga, M. P. Teulade-Fichou in *Visualizing the quadruplex: From fluorescent ligands to light-up probes, Vol. 330*, **2013**, pp. 111 – 178.
[46] a) F. Pan, C. Roland, C. Sagui, *Nucleic Acids Res.* **2014**, *42*, 13981 – 13996; b) A. A. Zinchenko, K. Yoshikawa, *Biophys. J.* **2005**, *88*, 4118 – 4123.

Manuscript received: April 30, 2018
Revised manuscript received: July 12, 2018
Version of record online: September 14, 2018